Life Sciences 234 (2019) 116789

Contents lists available at ScienceDirect

Life Sciences

journal homepage: www.elsevier.com/locate/lifescie

Long non-coding RNA Linc00483 accelerated tumorigenesis of cervical cancer by regulating miR-508-3p/RGS17 axis

Pin Hu[a], Guiju Zhou[a], Xiaohui Zhang[b], Geng Song[c], Lei Zhan[a], Yunxia Cao[b,*]

[a] Department of Obstetrics and Gynecology, The Second Affiliated Hospital of Anhui Medical University, Hefei, Anhui 230601, China
[b] Department of Obstetrics and Gynecology, The First Affiliated Hospital of Anhui Medical University, Hefei, Anhui 230022, China
[c] Departement of Oncology, The Second Affiliated Hospital of Anhui Medical University, Hefei, Anhui, 230601, China

ARTICLE INFO

Keywords:
Cervical cancer
Linc00483
miR-508-3p
RGS17
Tumorigenesis

ABSTRACT

Objectives: The aim of this study was to uncover the underlying mechanisms of cervical cancer progression and provide potential therapeutic targets for its treatment in clinic.
Materials and methods: Real-Time qPCR was used to determine the expression levels of Linc00483, miR-508-3p and RGS17 mRNA in cervical cancer tissues and cell lines. Terminal deoxynucleotidyl transferase (TdT)-mediated dUTP nick-end labeling (TUNEL) assay was conducted to determine cell apoptosis. Western Blot was performed to detect protein expression levels. Wound healing and Transwell assay were employed to determine cell migration and invasion respectively. Online software (TargetScan, miRDB and miR TarBase) were used to predict the regulating mechanisms of Linc00483, miR-508-3p and RGS17, which were validated by dual-luciferase reporter gene system. In vivo tumor-bearing mice models were established to validate the cellular results.
Results: Linc00483 aberrantly overexpressed in both cervical cancer tissues and cell lines comparing to the Control groups. Knock-down of Linc00483 inhibited cervical cancer cell proliferation, invasion as well as migration, and promoted cell apoptosis. In addition, miR-508-3p was identified as the downstream target of Linc00483, and miR-508-3p inhibitor abrogated the inhibiting effects of downregulated Linc00483 on cervical cancer cell viability. Furthermore, the expression levels of Linc00483 was positively correlated with RGS17 in the clinical samples and overexpressed Linc00483 increased RGS17 expression levels in cervical cancer cells by sponging miR-508-3p. The in vivo experiments showed that knock-down of Linc00483 inhibited cervical cancer cell tumorigenesis and lung metastasis in mice models.
Conclusions: Knock-down of Linc00483 inhibited the development of cervical cancer by regulating miR-508-3p/RGS17 axis.

1. Introduction

Cervical cancer is a common female malignancy [1] and there are still no effective therapies for its treatment in clinic [2–4]. The development of cervical cancer is complicated and current literatures agreed that human papillomavirus (HPV) infection was crucial for cervical cancer pathogenesis [5,6], and HPV encoded E6/E7 proteins were crucial for triggering cervical cancer pathogenesis [7–9]. Aside from HPV, LncRNAs have recently been reported to be crucial for the pathogenesis of cervical cancer [7]. Previous studies showed that LncRNA Linc00483 played an oncogenic role in lung adenocarcinoma [10], colorectal cancer [11] and gastric cancer [12], but it is still unclear whether Linc00483 participated in the development of cervical cancer. The preliminary results of this study showed that Linc00483 aberrantly overexpressed in cervical cancer tissues comparing to its paired normal adjacent tissues, which indicated that Linc00483 might also be an oncogene in cervical cancer.

It was commonly known that LncRNAs regulated cell functions and cancer development by sponging microRNAs (miRNAs) [13,14]. For example, LncRNA XIST promoted pancreatic cancer progression by sponging miR-429 [13] and LncRNA H19 promoted lung cancer metastasis by targeting miR-6515-3p [14]. Hence it is reasonable to speculate that Linc00483 might participate in the development of cervical cancer by targeting miRNAs. Studies showed that miR-508-3p was a tumor suppressor in multiple cancers, such as breast cancer [15], ovarian cancer [16] and gastric cancer [17]. However, the role of miR-508-3p in cervical cancer is still unclear. Of note, the online software predicted that miR-508-3p was the potential target of Linc00483. And

* Corresponding author at: Departement of Obstetrics and Gynecology , The First Affiliated Hospital of Anhui Medical University, No.218, Jixi Road, Shushan District, Hefei, Anhui, 230022, China.
E-mail address: YunxiaCaoswr@163.com (Y. Cao).

https://doi.org/10.1016/j.lfs.2019.116789
Received 17 July 2019; Accepted 23 August 2019
Available online 24 August 2019
0024-3205/

the preliminary experiments showed that Linc00483 was negatively correlated with miR-508-3p in cervical cancer tissues, hence Linc00483 might participate in cervical cancer progression by sponging miR-508-3p.

Regulator of G Protein Signaling 17 (RGS17) was an oncogene [18] and could be regulated by multiple miRNAs in cancer development [19]. For example, miR-199 inhibited malignant progression of lung cancer by targeting RGS17 [19] and miR-182 suppressed lung tumorigenesis through downregulating RGS17 expression levels [20], but it is still unclear whether RGS17 participated in the regulation of cervical cancer progression. Notably, the online software predicted that RGS17 was the potential downstream target of miR-508-3p, and RGS17 was positively correlated with Linc00483 levels in cervical cancer tissues. Therefore, Linc00484/miR-508-3p/RGS17 axis might be crucial for cervical cancer development, uncovering the underlying mechanisms will provide new therapeutic agents for cervical cancer treatment in clinic.

2. Materials and methods

2.1. Cervical cancer tissues

The cervical cancer tissue samples (N = 40) and its paired normal adjacent tissue samples (N = 40) were collected from patients diagnosed as cervical cancer from The Second Affiliated Hospital of Anhui Medical University. All the specimens were separated, collected and frozen at the refrigerator with −80 °C conditions. The average age of the patients was 51 ± 9.62 years old, specifically, 17 of them below 50 years old and 23 of them above 50 years old. In addition, 19 of them were at stage I–II and 21 of them were at stage III–IV. The detailed characteristics of the patients were listed in Table 2. All the clinical experiments in this study were in accordance with the principle of 'Declaration of Helsinki' [21] and approved by the ethics committee of The Second Affiliated Hospital of Anhui Medical University. All the patients have signed the inform consent.

2.2. Animal models

The 6-week nude mice (NU/NU) were purchased from Vital River Inc. (Beijing, China). For the tumor volume experiments, the SiHa cells were diluted to 1×10^6/200 μl by PBS and 200 μl of the above cell suspensions were subcutaneously injected into the left (Control group, PBS only) and right (experimental group, cell suspensions) flanks of the mice. The tumor growth was determined by using the formula $V = (L \times l^2)/2$, specifically, L and l represented the long and short diameters of the tumors. Besides, the tumor weight was evaluated by using electronic scales. For the metastasis experiments, the above cells were intravenously injected into mice by the lateral tail vein. After about 50 days, the mice were sacrificed and the lung tissues were separated and collected to determine cell metastasis abilities in vivo. All the experiments were approved by the Ethics Committee for Animal Experiments of The Second Affiliated Hospital of Anhui Medical University. The experiments were in accordance with the ethical standard of Helsinki Declaration of 1975, which was revised in 1983.

2.3. Cell culture and vectors transfection

Cervical cancer cell lines HeLa (#CRM-CCL-2), CaSki (#CRM-CRL-1550), C33A (#HTB-31), ME180 (#HTB-33) as well as SiHa (#HTB-35), and HEK-293T (#CRL-11268) cells were purchased from American Type Culture Collection (ATCC, USA). All the cells were cultured in Dulbecco's Modified Eagle Medium (DMEM) medium (Gibco, USA) with the conditions of 37 °C and humidified 5% CO_2 atmosphere. The sequence of Linc00483 was cloned into pcDNA3.1 vector to construct Linc00483 overexpressed vectors (OE-Linc00483) by Sangon Biotech (Shanghai, China). The small interfering RNAs (siRNAs) specifically targeting Linc00483 were purchased from Ribobio (Guangzhou, China). Besides, the miR-508-3p inhibitors were designed and constructed by Sangon Biotech (Shanghai, China). The above vectors were transfected in cervical cancer cells and HEK-293T cells by using Lipofectamine obtained from Invitrogen (CA, USA) according to the manufacturer's protocol.

Table 1
Primer sequences for Real-Time qPCR.

Gene	Primer sequences (strand)
β-Actin	Forward: 5′-CTCCATCCTGGCCTCGCTGT-3′ Reverse: 5′-GCTGCTACCTTCACCGTTCC-3′
Linc00483	Forward: 5′-GCTGAACCGGAACAGGACAT-3′ Reverse: 5′-CCAGTTCACAGCAACTCACG-3′
RGS17	Forward: 5′-CAGAGCTCATGCGAAAAAGGCAG-3′ Reverse: 5′-GGTCTAGATAAATGAACATTAAG-3′
U6	Forward: 5′-CTCGCTTCGGCAGCACA-3′ Reverse: 5′-AACGCTTCACGAATTTGCGT-3′
miR-508-3p	Forward: 5′-CAAGCATGATTGTAGCCTTTTG-3′ Reverse: 5′-TATCGTTGTACTCCAGACCAAGAC-3′

2.4. Real-Time qPCR

The cervical cancer tissues and cell lines were collected and prepared for further treatment. The total RNA of the above clinical and cellular samples was extracted by Trizol kit purchased from Invitrogen (USA) according to the manufacturer's instruction. The total RNA was then reversely transcribed into complementary DNA (cDNA) by using a RT-PCR kit obtained from Promega (USA). Finally, a Real-Time qPCR kit purchased from QIAGEN (Germany) was used to determine the mRNA levels of the associated genes in this study. The primer subsequences were listed in Table 1.

2.5. Western Blot

The RIPA lysis buffer (Beyotime Biotechnology, Shanghai, China) was used to extract the total proteins from cervical cancer tissues and cell lines. The 10% SDS-polyacrylamide gel (SDS-PAGE) was employed to separate the protein bands and the selected bands were then transferred to polyvinylidene fluoride (PVDF) membranes (Millipore, Bedford, MA, USA). The primary antibodies including anti-RGS17 (1:1000, #ab96675, Abcam, UK), anti-GAPDH (1:2000, #ab8226, Abcam, UK), anti-p21 (1:1500, #ab218311, Abcam, UK), anti-Cyclin D1 (1:1000, #ab134175, Abcam, UK), anti-p27 (1:1000, #ab32034, Abcam, UK), anti-Bcl-2 (1:1000, #ab32124, Abcam, UK), anti-Bax (1:1000, #ab53154, Abcam, UK), anti-Caspase 3 (1:1000, #ab32351, Abcam, UK), anti-E-cadherin (1:1500, #ab15148, Abcam, UK), anti-MMP9 (1:2000, #ab38898, Abcam, UK), anti-Vimentin (1:1000, #ab193555, Abcam, UK) and anti-MMP2 (1:1500, #ab37150, Abcam, UK) were probed with the PVDF membranes for 2 h at the room temperature. Subsequently, the membranes were incubated with the horseradish peroxidase (HRP)-conjugated secondary antibody (Abcam) for 1 h at room temperature. Finally, the ECL Western Blotting Detection Kit was purchased from Healthcare Bio-Science (PA, USA) to detect the protein bands, which were then quantified by Image J software.

2.6. Terminal deoxynucleotidyl transferase (TdT)-mediated dUTP nick-end labeling (TUNEL) assay

The TUNEL apoptosis assay kit (Beyotime, Shanghai, China) was purchased to detect cell apoptosis according to the manufacturer's protocol. Briefly, the cervical cancer cells were washed with phosphate buffer solution (PBS) for three times and fixed with 4% paraformaldehyde for 30 min. The PBS containing 0.3% Triton X-100 was incubated

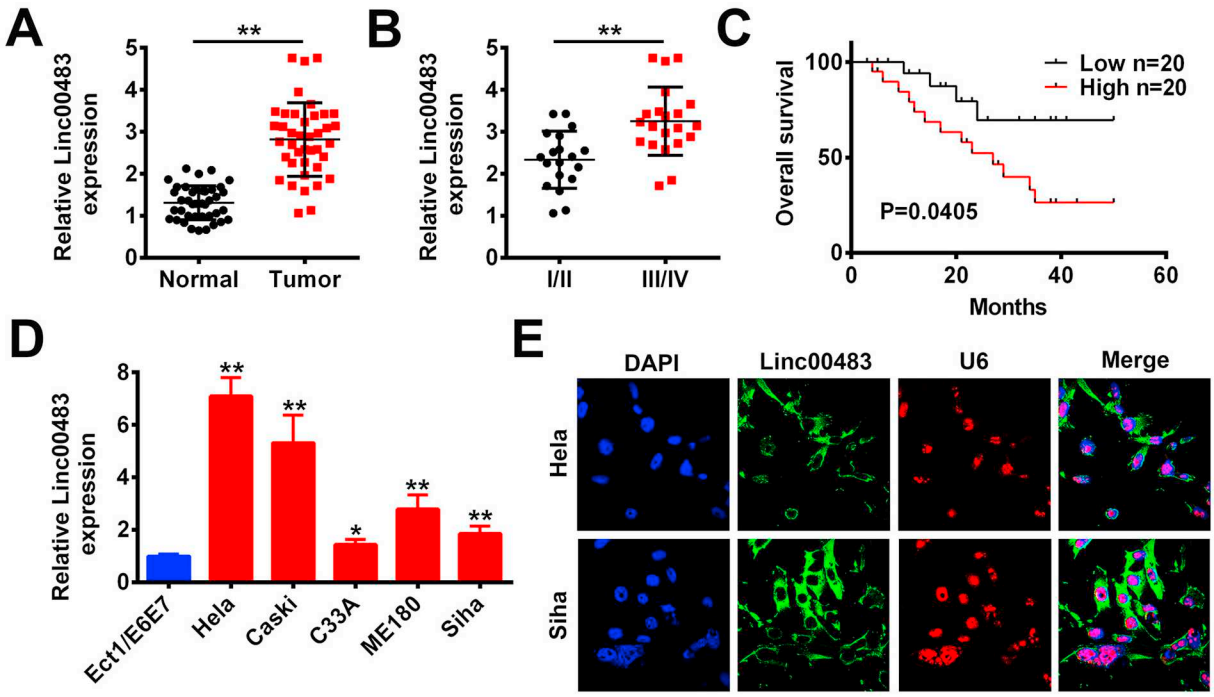

Fig. 1. The expression levels of Linc00483 in cervical cancer tissues and cell lines.
(A, B) Relative Linc00483 expressions in cervical cancer tissues were determined by Real-Time qPCR. (C) Kaplan-Meier analysis was performed to analyze the correlation between overall survival and Linc00483 levels in cervical cancer patients. (D) Relative Linc00483 expressions in different cervical cancer cell lines. (E) RNA-FISH was used to detect expressions and localization of Linc00483 in cervical cancer cells. "*" means $p < 0.05$, "**" means $p < 0.01$.

with the above cells for 5 min at room temperature. The TUNEL detection solution was then added and FCM was used to detect cell apoptosis ratio.

2.7. Wound healing assay

The cervical cancer cells were diluted and seeded into 6-well plates until the confluency reached about 80%. The Eppendorf tip was used to scratch in the cell monolayer. After that, an Olympus microscope was used to record the scratch wounds in the same position at 0 h and 24 h respectively. The Image J software was used to quantify the denuded areas. Each experiment was repeated at least 3 times.

2.8. Transwell assay

The transwell chambers (Corning, NY, USA) was used to detect cell invasion. In brief, cells were seeded into the matrigel-coated upper chamber with FBS free DMEM medium at the concentration of 1 mg/ml. After the cell confluency reached about 80%, the DMEM medium with 10% fetal calf serum (FBS) was added into the lower chamber and cultured for 24 h. The invasive cells were then fixed with 4% paraformaldehyde and stained with 0.5% crystal violet for 30 min. The Olympus microscope was used to count invading cell numbers to evaluate cell invasion ability.

2.9. Dual-luciferase reporter gene system

The fragments from Linc00483 and RGS17 containing the binding sites of miR-508-3p or the corresponding mutants were cloned into a pmiRGLO Vector (Promega, WI, USA). The above vectors, miR-508-3p mimic and inhibitor were co-transfected into HEK-293T cells by using Lipofectamine 2000 (Invitrogen, USA). The dual-luciferase reporter gene system (Promega, USA) was employed to detect luciferase activities according to the manufacturer's instruction.

2.10. Hematoxylin-eosin (HE) staining

The mice lung tissues were collected and fixed with 10% formalin for 48 h. After that, the 5% nitric acid solution was used to decalcificate the samples for 24 h and paraffin embedding was next conducted. The ultra-thin semiautomatic microtome (Shandon, UK) was used to generate paraffin sections of 3 μm in thickness and were baked for 1 h at 45 °C. The HE staining was then performed to stain the sections and a microscope (Leica Microsystems Inc., Germany) was used to observe tissue morphology.

2.11. Immunohistochemistry (IHC)

The mice tumor tissues collected and the paraffin embedded sections were prepared. The specimens were then de-paraffinized and rinsed in PBS. Antigen retrieval was then performed and the primary antibodies including anti-ki67 (1:1000, #ab15580, Abcam, UK), RGS17 (1:1000, #ab96675, Abcam, UK) and Vimentin (1:500, #ab193555, Abcam, UK) were incubated with the sections. After that, the secondary antibody was probed with the specimens and a 3,3′-diaminobenzidine (DAB) kit (Sangon Biotech Co., Ltd., Shanghai, China) was used to determine the expression levels and localization of the target proteins.

2.12. Statistical analysis

All the data were collected and expressed as the Mean ± Standard Deviation (SD) from the experiments repeated at least three times and analyzed by using SPSS 17.0 software (SPSS, Chicago, Illinois, USA). The Student's *t*-test was used to compare two groups. The Analysis of Variance (ANOVA) was used for analyzing the statistical significances of multiple groups. The Kaplan-Meier method was employed to generate survival curves and log-rank test was used to analyze the differences. $p < 0.05$ was considered statistically significant.

Table 2
Characteristics of cervical cancer patients. The correlations among Linc00483 levels and patient age, clinical stage, tumor size, distant metastasis, histological type and histological grade were analyzed.

Characteristics	n	Relative Linc00483 expression		p
		High	Low	
Age (years)				0.749
≤50	17	9	8	
> 50	23	11	12	
Clinical stage				0.004
I–II	19	5	14	
III–IV	21	15	6	
Tumor size (cm)				0.013
≤4	29	18	11	
> 4	11	2	9	
Distant metastasis				0.004
Absent	36	16	20	
Present	4	4	0	
Histological type				0.147
Adenocarcinoma	2	2	0	
Squamous cell carcinoma	38	18	20	
Histological grade				0.342
Well	19	8	11	
Moderately/poorly	21	12	9	

3. Results

3.1. The expression levels of Linc00483 in cervical cancer tissues and cell lines

The cervical cancer and adjacent normal tissues were collected, the results showed that Linc00483 overexpressed in tumor tissues comparing to the normal tissues (Fig. 1A). Besides, the expression levels of Linc00483 were higher in tumor tissues collected from the patients with staging III/IV, tumor size (> 4) and distant metastasis (Present) than their counterparts (Fig. 1B, Table 2), but had nothing to do with patient age, tumor histological type and grade (Table 2). The expression levels of Linc00483 were negatively correlated with overall survival of cervical cancer patients (Fig. 1C). Furthermore, the cellular results showed that Linc00483 levels were higher in cervical cancer cell lines (HeLa, CaSki, C33A, ME180 and SiHa) than the immortalized cervical squamous cell line (Ect1/E6E7) (Fig. 1D). The RNA-FISH results also showed that Linc00483 highly expressed in HeLa as well as SiHa cells, and mainly localized in cytoplasm instead of nucleus (Fig. 1E). Since Linc00483 was comparatively low expressed in C33A and SiHa cells comparing to the Hela and CaSki cells, further experiments overexpressed Linc00483 in C33A and SiHa cells, and downregulated Linc00483 in HeLa and CaSki cells.

3.2. Effects of Linc00483 on cervical cancer cell proliferation and apoptosis

The overexpressed vectors of Linc00483 were transfected into C33A and SiHa cells (Fig. 2A). Besides, the knock-down vectors of Linc00483 were transfected into HeLa and CaSki cells (Fig. 2C). Overexpressed Linc00483 increased C33A and SiHa cell proliferation (Fig. 2B). Similarly, knock-down of Linc00483 inhibited HeLa and CaSki cell proliferation (Fig. 2D). In addition, overexpressed Linc00483 upregulated cyclin D1 and downregulated p21 as well as p27 in C33A and SiHa cells (Fig. 2F), which were all reversed by knocking down Linc00483 in HeLa and CaSki cells (Fig. 2F). The TUNEL results showed that overexpressed Linc00483 decreased C33A as well as SiHa cell apoptosis ratio, which were increased by knocking down Linc00483 in Hela and CaSki cells (Fig. 2E). Furthermore, overexpressed Linc00483 decreased Bax as well as Caspase 3, and increased Bcl-2 levels in C33A and SiHa cells (Fig. 2F), and knock-down of Linc00483 had opposite effects on the above proteins in HeLa and CaSki cells (Fig. 2F). The above results indicated that Linc00483 promoted cervical cancer cell proliferation and inhibited cell apoptosis.

3.3. Influences of Linc00483 on cervical cancer cell invasion and migration

The Wound healing results showed that overexpressed Linc00483 increased C33A as well as SiHa cell migration, and knock-down of Linc00483 decreased HeLa as well as CaSki cell migration accordingly (Fig. 3A). Similarly, the Transwell assay results showed that overexpressed Linc00483 increased C33A as well as SiHa cell invasion, and knock-down of Linc00483 decreased HeLa as well as CaSki cell invasion accordingly (Fig. 3B). In addition, overexpressed Linc00483 decreased E-cadherin and increased MMP9, Vimentin and MMP2 in C33A and SiHa cells (Fig. 3C). The expression levels of E-cadherin were increased and MMP9, Vimentin as well as MMP2 were decreased by knocking down Linc00483 in HeLa and CaSki cells (Fig. 3C). The above results indicated that Linc00483 promoted epithelial-mesenchymal transition (EMT) of cervical cancer cells, and promoted cell invasion and migration.

3.4. Linc00483 inhibited miR-508-3p levels in cervical cancer cells by binding to its 3′UTR regions

The online miRDB software (http://mirdb.org/) predicted the potential binding sites of miR-508-3p and Linc00483, and the binding sites in Linc00483 were further mutated (Fig. 4A). The dual-luciferase reporter gene system results showed that miR-508-3p mimic transfection successfully decreased relative luciferase activity in HEK-293 T cells transfected with wild type Linc00483 instead of the mutated counterpart (Fig. 4A). Besides, the RNA-pull down results showed that miR-508-3p was prone to be enriched in Linc00483 group instead of the mock group (Fig. 4B). In addition, overexpressed Linc00483 decreased miR-508-3p levels in C33A as well as SiHa cells, and miR-508-3p levels were increased by knocking down Linc00483 in HeLa as well as CaSki cells (Fig. 4C). Furthermore, the levels of miR-508-3p in cervical cancer tissues was lower than its paired normal adjacent tissues (Fig. 4D), which were negatively correlated with Linc00483 levels in clinical samples (Fig. 4E).

3.5. RGS17 was targeted by miR-508-3p in cervical cancer cells

The online software (Targetscan, miRDB and miR TarBase) predicted that RGS17 was the overlapping potential downstream target of miR-508-3p (Fig. 5A), and the binding sites of miR-508-3p and RGS17 mRNA were also determined, which were further mutated in RGS17 mRNA (Fig. 5B). Further results showed that miR-508-3p mimic decreased luciferase activity in HEK-293T cells, which was increased by miR-508-3p inhibitor (Fig. 5B). In addition, miR-508-3p mimic inhibited RGS17 expressions in CaSki cells, and miR-508-3p inhibitor increased the expression levels of RGS17 in SiHa cells (Fig. 5C, D). The clinical results also showed that RGS17 aberrantly overexpressed in cervical cancer tissues comparing to the normal adjacent tissues (Fig. 5E–G). Furthermore, the expression levels of miR-508-3p were negatively correlated with RGS17, and Linc00483 was positively correlated with RGS17 in cervical cancer tissues (Fig. 5H).

3.6. Linc00483 affected cervical cancer cell proliferation, apoptosis, invasion and migration by sponging miR-508-3p

The MTT assay results showed that knock-down of Linc00483 inhibited HeLa and CaSki cell proliferation, which were reversed by synergistically transfecting cells with miR-508-3p inhibitor (Fig. 6A). Besides, the TUNEL assay results showed that knock-down of Linc00483 increased HeLa and CaSki cell apoptosis ratio, which was abrogated by downregulating miR-508-3p (Fig. 6B). Similarly, downregulated Linc00483 also inhibited HeLa and CaSki cell migration and invasion,

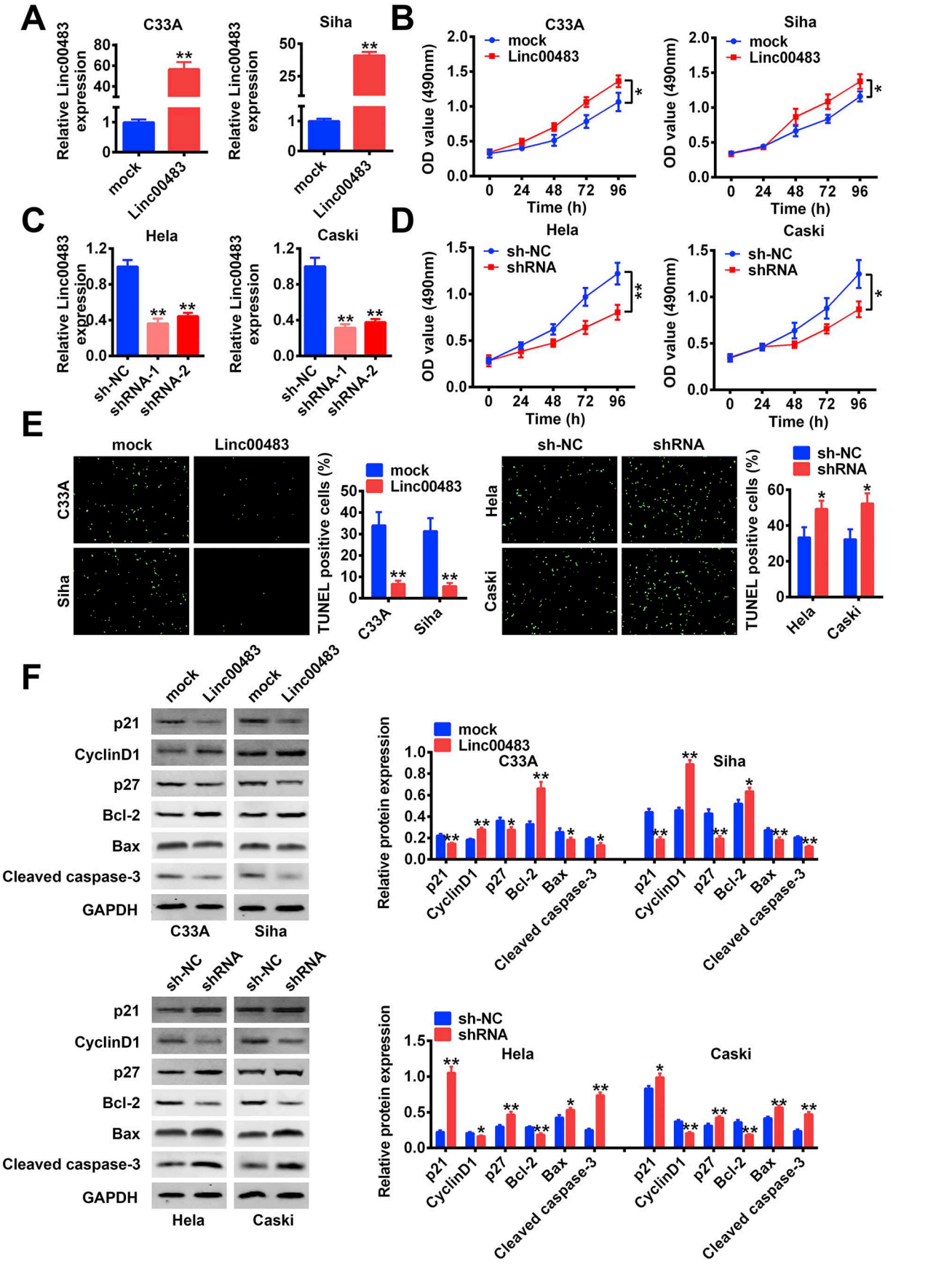

Fig. 2. The effects of Linc00483 on cervical cancer cell proliferation and apoptosis.
(A) Real-Time qPCR was used to determine Linc00483 levels in C33A, SiHa, HeLa and CaSki cells. (B) MTT assay was conducted to detect cervical cancer cell viability. (C) TUNEL assay was performed to detect cervical cancer cell apoptosis ratio. (D) Western Blot was employed to detect the expressions of p21, Cyclin D1, p27, Bcl-2, Bax, cleaved caspase 3 in cervical cancer cells. "*" means $p < 0.05$, "**" means $p < 0.01$.

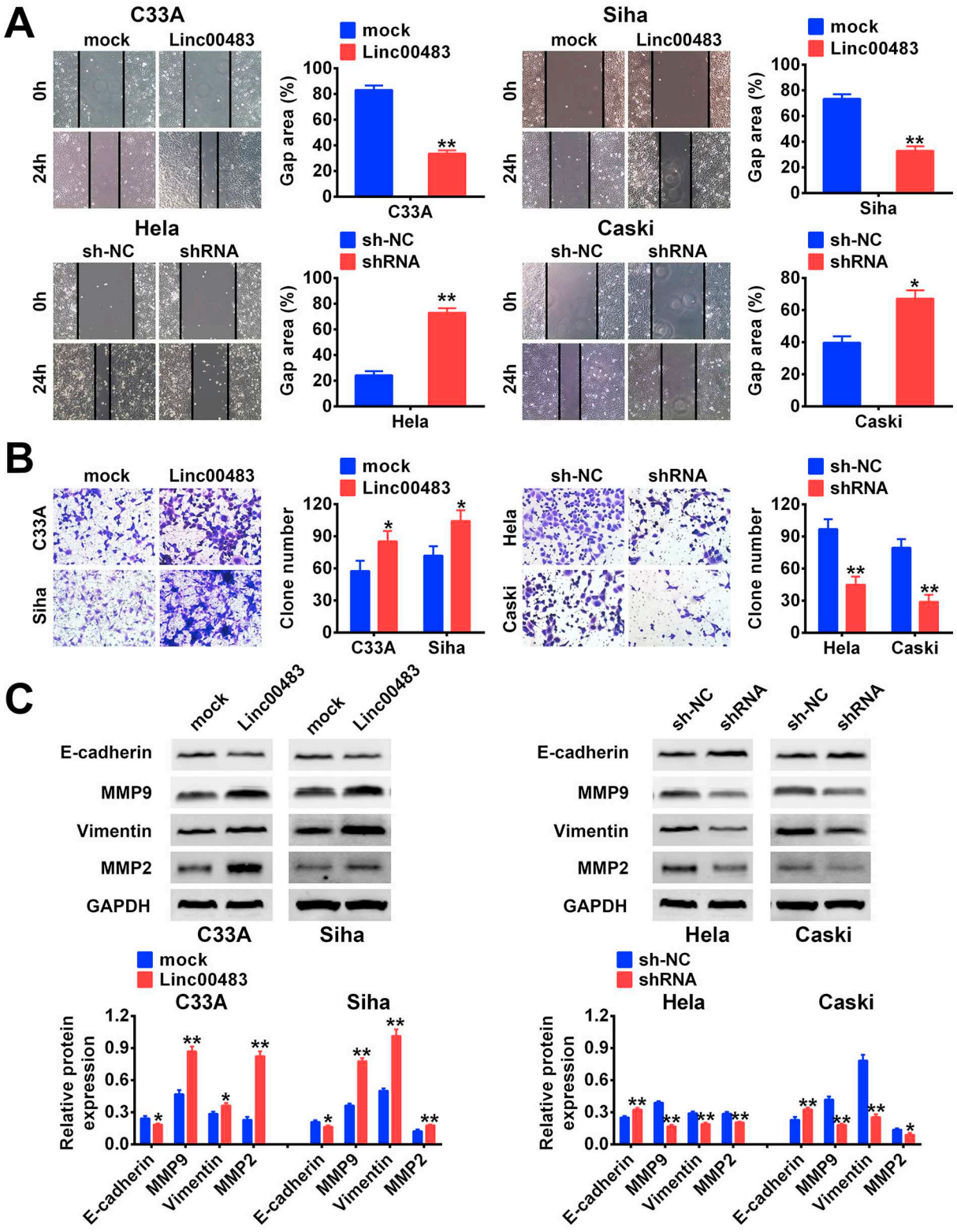

Fig. 3. The effects of Linc00483 on cervical cancer cell invasion and migration.
(A) Wound healing assay was used to detect cervical cancer cell migration ability. (B) Transwell assay was employed to determine cervical cancer cell invasion ability. (C) Western Blot was conducted to detect the expressions of E-cadherin, MMP9, Vimentin and MMP2 in cervical cancer cells. "*" means $p < 0.05$, "**" means $p < 0.01$.

which were all restored by synergistically knocking down miR-508-3p (Fig. 6C, D). In addition, the effects of downregulated Linc00483 on the expression levels of protein associated proteins (p21, Cyclin D1 andp27), apoptosis associated proteins (Bcl-2, Bax andCaspase3) and EMT associated proteins (E-cadherin, MMP9, Vimentin and MMP2) were all abrogated by miR-508-3p inhibitor (Fig. 6E). Of note, the results showed that Linc00483 increased RGS17 expression levels by targeting miR-508-3p (Fig. 6E).

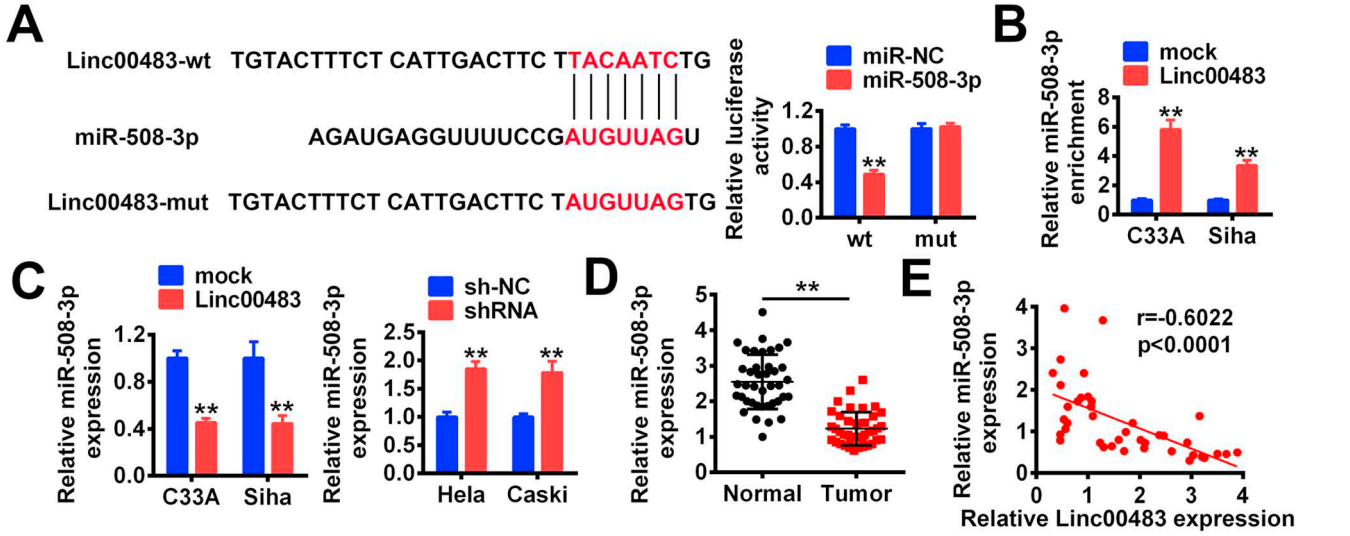

Fig. 4. The interactions between Linc00483 and miR-508-3p.
(A) The biding sites of Linc00483 and miR-508-3p was predicted by online miRDB software and validated by dual-luciferase reporter gene system. (B) RNA-pull down assay was performed to detect miR-508-3p enrichment in Linc00483. (C) The effects of Linc00483 on miR-508-3p levels in cervical cancer cells. (D) The expression levels of miR-508-3p in cervical cancer tissues. (E) The correlation analysis of Linc00483 and miR-508-3p levels in cervical cancer tissues. "*" means $p < 0.05$, "**" means $p < 0.01$.

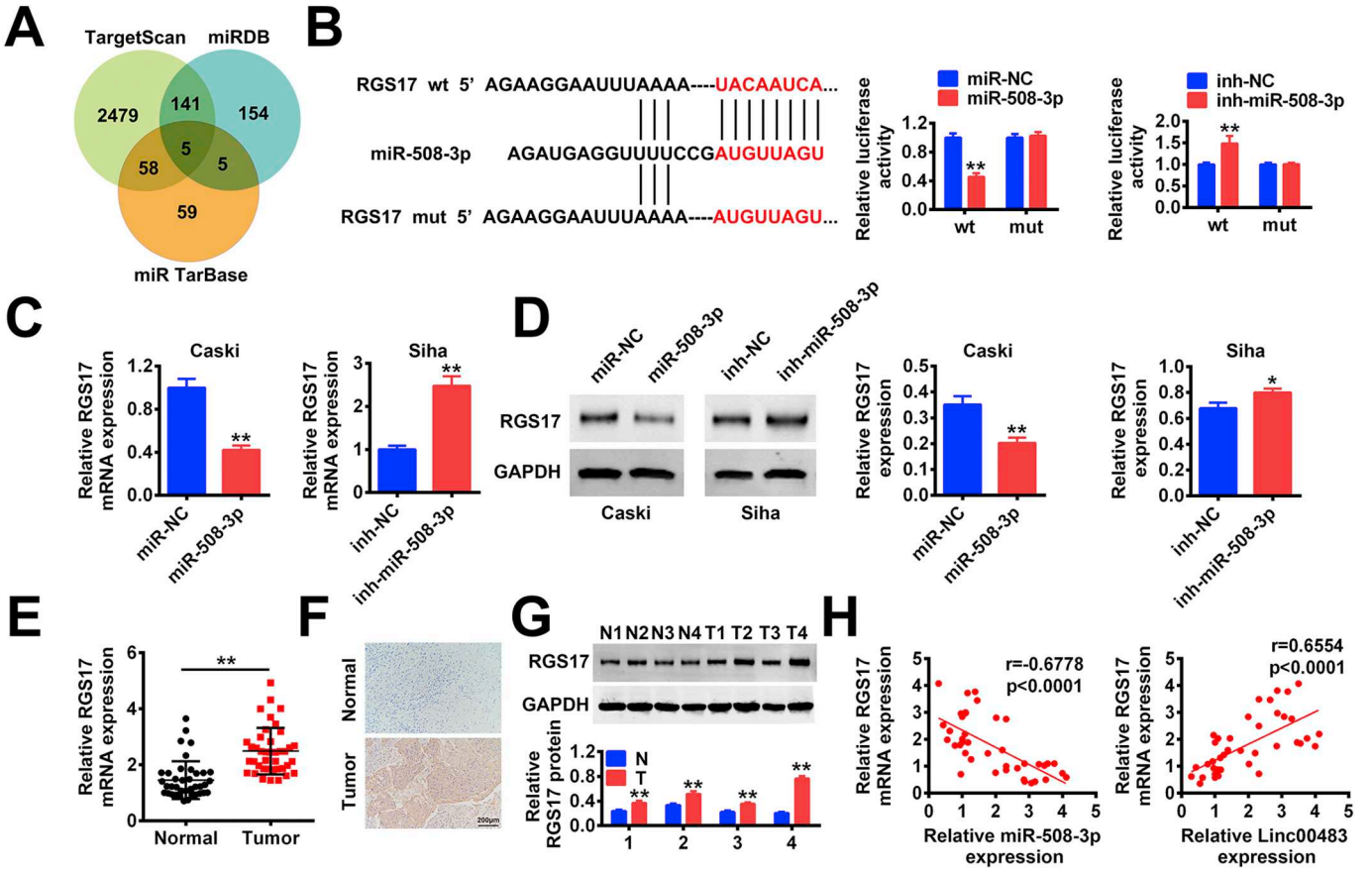

Fig. 5. The levels of RGS17 were regulated by miR-508-3p.
(A) The online software (TargetScan, miRDB and miR TarBase) were used to predict the potential downstream targets of miR-508-3p. (B) The regulating relationship of miR-508-3p and RGS17 was investigated by dual-luciferase reporter gene system. (C) Real-Time qPCR was used to determine RGS17 mRNA levels in CaSki and SiHa cells. (D) Western Blot was used to detect RGS17 expression levels in CaSki and SiHa cells. (E) Real-Time qPCR was used to determine RGS17 mRNA levels in cervical cancer tissues. (F) IHC was used to determine the expressions and localization of RGS17 in cervical cancer tissues. (G) Western Blot was performed to detect RGS17 expression levels in cervical cancer tissues. (H) The correlation analysis of Linc00483, miR-508-3p and RGS17 mRNA levels in cervical cancer tissues. "*" means $p < 0.05$, "**" means $p < 0.01$.

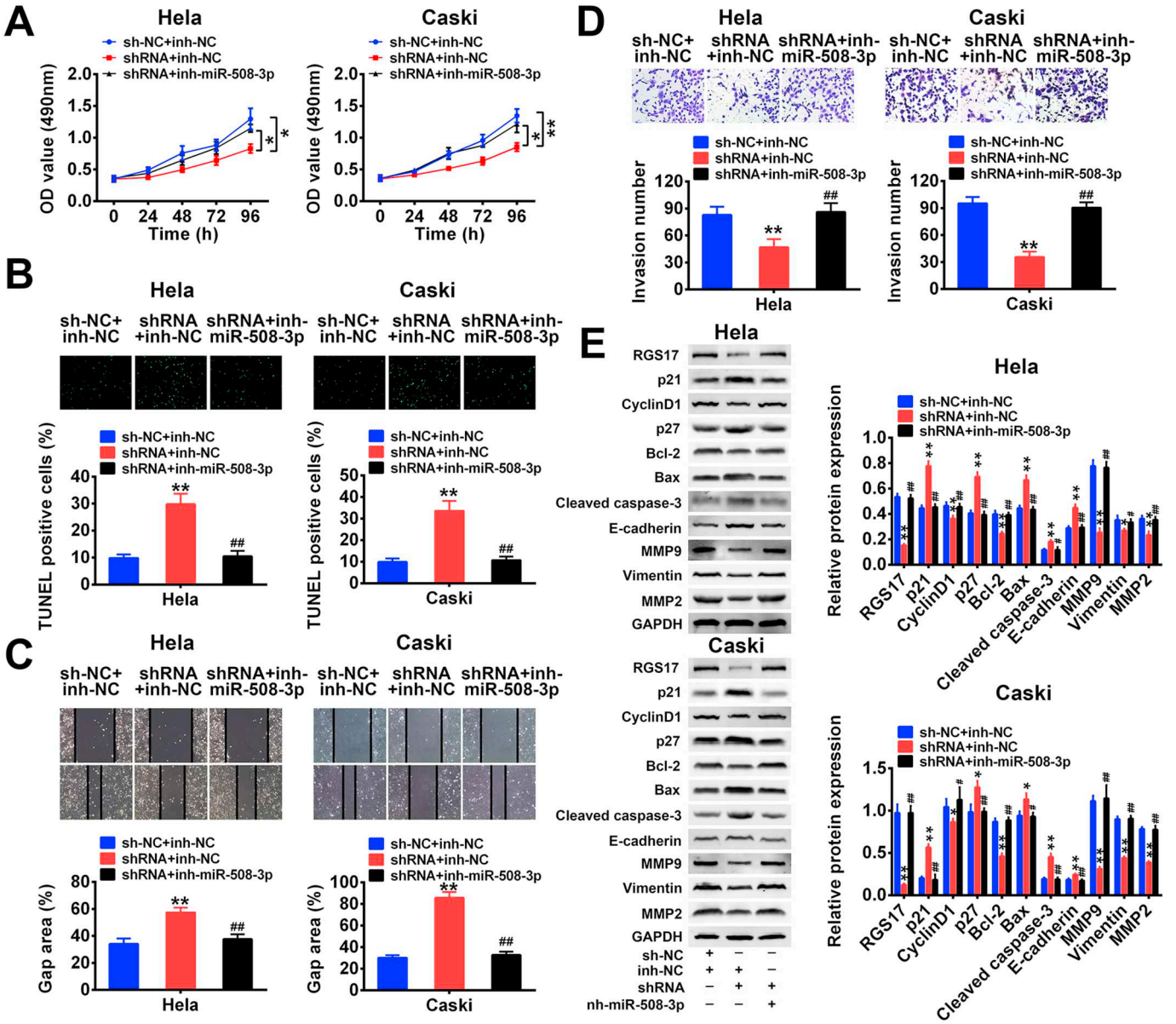

Fig. 6. The effects of Linc0048/miR-508-3p axis on cervical cancer cell proliferation, apoptosis, invasion and migration.
(A) MTT assay was used to detect HeLa and CaSki cell proliferation. (B) TUNEL assay was used to detect HeLa and CaSki cell apoptosis. (C) Wound healing assay was performed to determine HeLa and CaSki cell migration. (D) Transwell assay was conducted to detect HeLa and CaSki cell invasion. (E) Western Blot was employed to detect RGS17, p21, Cyclin D1, p27, Bcl-2, Bax, Caspase 3, E-cadherin, MMP9, Vimentin and MMP2 expressions in HeLa and CaSki cells. "*" means $p < 0.05$, "**" means $p < 0.01$.

3.7. Knock-down of Linc00483 inhibited cervical cancer cell tumorigenesis in mice models

The in vivo tumor volume experiments were conducted to investigate the effects of Linc00483 on cervical cancer cell tumorigenesis in mice models. The results showed that knock-down of Linc00483 inhibited tumor volume and weight in tumor-bearing mice (Fig. 7A, B). Besides, knock-down of Linc00483 inhibited expressions of ki67, RGS17 and Vimentin in mice tumor tissues (Fig. 7C). Further results also showed that knock-down of Linc00483 upregulated miR-508-3p levels (Fig. 7D) and increased cell apoptosis ratio (Fig. 7E) in mice tumors. In addition, the in vivo tumor metastasis models were also inducted in nude mice, the HE staining results showed that knock-down of Linc00483 significantly decreased tumor numbers in mice lung tissues and inhibited cell metastasis in mice models (Fig. 7F).

4. Discussion

The complexity of cervical cancer pathogenesis seriously limited its researching and treatment in clinic [22], uncovering the underlying mechanisms might help to solve this problem. Recent studies have reported that the aberration of long non-coding RNAs (LncRNAs) was closely related to the development of cervical cancer [23,24] and identification of LncRNAs might provide potential therapeutic agents for cancer treatment in clinic. The preliminary experiments of this study filtered that Linc00483 was significant overexpressed in both cervical cancer tissues as well as cell lines comparing to the Control groups, and negatively correlated with patients prognosis. Besides, knock-down of Linc00483 inhibited cervical cancer cell proliferation, migration as well as invasion, and promoted cell apoptosis, which were in accordance with the previous studies and showed that Linc00483 was an oncogene and promoted the development of lung adenocarcinoma [10],

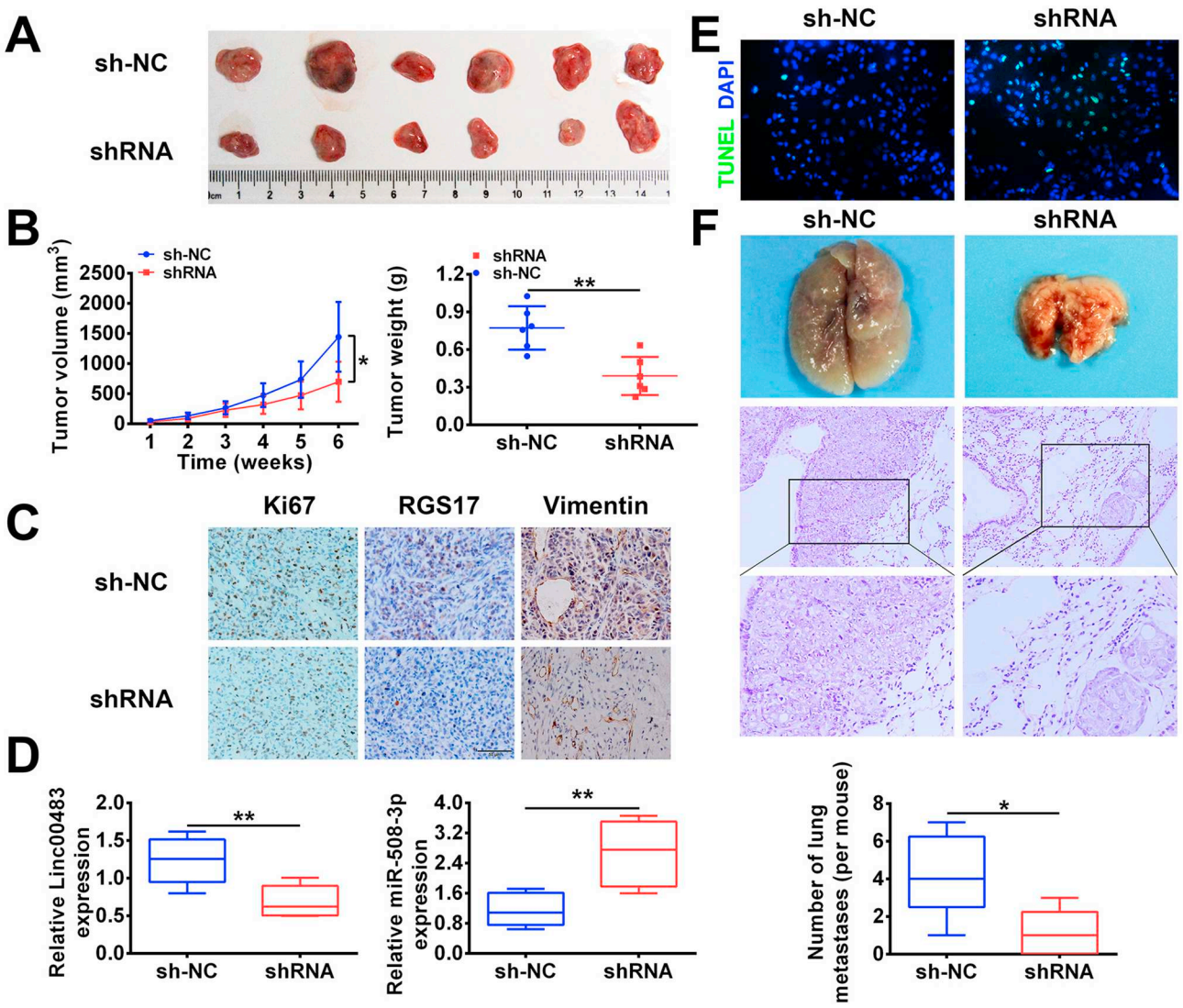

Fig. 7. The effects of Linc00483 on HeLa cell tumorigenesis in mice models.
(A) Mice tumors were collected and photographed. (B) Tumor volume and weight were measured respectively. (C) IHC was used to determine Ki67, RGS17 and Vimentin localization and expression levels in mice tumor tissues. (D) Real-Time qPCR was used to detect levels of Linc00483 and miR-508-3p in mice tumor tissues. (E) TUNEL assay was performed to detect cell apoptosis in mice tumor tissues. (F) HE staining was employed to determine pulmonary metastasis of HeLa cells in mice models. "*" means $p < 0.05$, "**" means $p < 0.01$.

colorectal cancer (CRC) [11] and gastric cancer (GC) [12]. Furthermore, the in vivo experiments showed that knock-down of Linc00483 inhibited tumor growth and lung metastasis in mice models, which indicated that overexpressed Linc00483 promoted cervical cancer progression, and Linc00483 played an oncogenic role in the development of cervical cancer.

The Online software (TargetScan, miRDB and miR TarBase) predicted that miR-508-3p was the downstream target of Linc00483, which was validated in further experiments. Previous studies showed that miR-508-3p served as a tumor suppressor in multiple cancers including breast cancer [15], gastric cancer [17] and renal cell carcinoma [25], but the relationship between miR-508-3p and cervical cancer is still not understood. The results in this study showed that miR-508-3p inhibited cervical cancer cell proliferation and metastasis, and promoted cell apoptosis, which indicated that miR-508-3p inhibited cervical cancer progression and in line with the previous study [15]. In addition, knock-down of Linc00483 inhibited cervical cancer cell proliferation, migration as well as invasion, and promoted cell apoptosis, which were all reversed by synergistically knocking down miR-508-3p. The results suggested that downregulated Linc00483 inhibited cervical cancer progression by targeting miR-508-3p.

Previous studies showed that overexpressed RGS17 promoted the development of multiple cancers [18] and indicated that targeting RGS17 might me a novel therapeutic agents for lung cancer [19]. However, whether RGS17 participated in cervical cancer progression is still unknown. This study found that RGS17 aberrantly overexpressed in cervical cancer tissues and cell lines comparing to the control groups. Further results also showed that RGS17 expressions were negatively correlated with miR-508-3p, and positively correlated with Linc00483. Notably, RGS17 was the downstream target of miR-508-3p, and this study showed that Linc00483 regulated RGS17 expressions by targeting miR-508-3p, which indicated that RGS17 was an oncogene in cervical cancer and was in accordance with the previous studies in lung cancer [19], hepatocellular carcinoma [26] and non-small cell lung cancer [27]. In addition, the in vivo experiments were in line with the cellular results, which showed that knock-down of miR-508-3p abrogated the effects of downregulated Linc00483 on tumorigenesis and metastasis of cervical cancer cells. The above results indicated that Linc00483 participated in cervical cancer cell proliferation, apoptosis, invasion, migration and tumorigenesis by regulating miR-508-3p/RGS17 axis.

Taken together, this study validated that Linc00483 promoted cervical cancer progression by targeting miR-508-3p/RGS17 axis and will provide new therapeutic agents for cervical cancer treatment in clinic.

Availability of data and materials

All data generated or analyzed during this study are included in this published article.

Acknowledgements

Not applicable.

Funding

Not applicable.

Declaration of competing interest

The authors declare that they have no competing interests, and all authors should confirm its accuracy.

Authors' contributions

PH and YXC conceived and designed the experiments, GJZ and XHZ analyzed and interpreted the results of the experiments, GS and LZ performed the experiments.

Ethics approval and consent to participate

The animal use protocol listed below has been reviewed and approved by the Animal Ethical and Welfare Committee.

References

[1] P. Tsikouras, S. Zervoudis, B. Manav, E. Tomara, G. Iatrakis, C. Romanidis, et al., Cervical cancer: screening, diagnosis and staging, J. BUON 21 (2) (2016) 320–325.
[2] G. Menderes, J. Black, C.L. Schwab, A.D. Santin, Immunotherapy and targeted therapy for cervical cancer: an update, Expert. Rev. Anticancer. Ther. 16 (1) (2016) 83–98.
[3] J. Fang, H. Zhang, S. Jin, Epigenetics and cervical cancer: from pathogenesis to therapy, Tumour Biol. 35 (6) (2014) 5083–5093.
[4] M. Takekuma, Y. Kasamatsu, N. Kado, S. Kuji, A. Tanaka, N. Takahashi, et al., The issues regarding postoperative adjuvant therapy and prognostic risk factors for patients with stage I-II cervical cancer: a review, J. Obstet. Gynaecol. Res. 43 (4) (2017) 617–626.
[5] S. Fukui, K. Nagasaka, N. Iimura, R. Kanda, T. Ichinose, T. Sugihara, et al., Detection of HPV RNA molecules in stratified mucin-producing intraepithelial lesion (SMILE) with concurrent cervical intraepithelial lesion: a case report, Virol. J. 16 (1) (2019) 76.
[6] E. Reeves, O. Wood, C.H. Ottensmeier, E.V. King, G.J. Thomas, T. Elliott, et al., HPV epitope processing differences correlate with ERAP1 allotype and extent of CD8+ T cell tumor infiltration in OPSCC, Cancer Immunol. Res. 7 (7) (2019) 1202–1213.
[7] J.A. Barr, K.E. Hayes, T. Brownmiller, A.D. Harold, R. Jagannathan, P.R. Lockman, et al., Long non-coding RNA FAM83H-AS1 is regulated by human papillomavirus 16 E6 independently of p53 in cervical cancer cells, Sci. Rep. 9 (1) (2019) 3662.
[8] H. He, X. Liu, Y. Liu, M. Zhang, Y. Lai, Y. Hao, et al., Human papillomavirus E6/E7 and long noncoding RNA TMPOP2 mutually upregulated gene expression in cervical cancer cells, J. Virol. 93 (8) (2019).
[9] S. Sharma, K. Munger, Expression of the cervical carcinoma expressed PCNA regulatory (CCEPR) long noncoding RNA is driven by the human papillomavirus E6 protein and modulates cell proliferation independent of PCNA, Virology 518 (2018) 8–13.
[10] Q.S. Yang, B. Li, G. Xu, S.Q. Yang, P. Wang, H.H. Tang, et al., Long noncoding RNA LINC00483/microRNA-144 regulates radiosensitivity and epithelial-mesenchymal transition in lung adenocarcinoma by interacting with HOXA10, J. Cell. Physiol. 234 (7) (2019) 11805–11821.
[11] Y. Yan, Z. Wang, B. Qin, A novel long noncoding RNA, LINC00483 promotes proliferation and metastasis via modulating of FMNL2 in CRC, Biochem. Biophys. Res. Commun. 509 (2) (2019) 441–447.
[12] D. Li, M. Yang, A. Liao, B. Zeng, D. Liu, Y. Yao, et al., Linc00483 as ceRNA regulates proliferation and apoptosis through activating MAPKs in gastric cancer, J. Cell. Mol. Med. 22 (2018) 3875–3886.
[13] J. Shen, L. Hong, D. Yu, T. Cao, Z. Zhou, S. He, LncRNA XIST promotes pancreatic cancer migration, invasion and EMT by sponging miR-429 to modulate ZEB1 expression, Int. J. Biochem. Cell Biol. 113 (2019) 17–26.
[14] Y. Xu, J. Lin, Y. Jin, M. Chen, H. Zheng, J. Feng, The miRNA hsa-miR-6515-3p potentially contributes to lncRNA H19-mediated-lung cancer metastasis, J. Cell. Biochem. (2019) 17413–17421.
[15] S.J. Guo, H.X. Zeng, P. Huang, S. Wang, C.H. Xie, S.J. Li, MiR-508-3p inhibits cell invasion and epithelial-mesenchymal transition by targeting ZEB1 in triple-negative breast cancer, Eur. Rev. Med. Pharmacol. Sci. 22 (19) (2018) 6379–6385.
[16] C.K. Chan, Y. Pan, K. Nyberg, M.A. Marra, E.L. Lim, S.J. Jones, et al., Tumour-suppressor microRNAs regulate ovarian cancer cell physical properties and invasive behaviour, Open Biol. 6 (11) (2016).
[17] T. Huang, W. Kang, B. Zhang, F. Wu, Y. Dong, J.H. Tong, et al., miR-508-3p concordantly silences NFKB1 and RELA to inactivate canonical NF-kappaB signaling in gastric carcinogenesis, Mol. Cancer 15 (2016) 9.
[18] L. Li, H.S. Luo, G-protein signaling protein-17 (RGS17) is upregulated and promotes tumor growth and migration in human colorectal carcinoma, Oncol. Res. 26 (1) (2018) 27–35.
[19] W.Z. Su, L.F. Ren, MiRNA-199 inhibits malignant progression of lung cancer through mediating RGS17, Eur. Rev. Med. Pharmacol. Sci. 23 (8) (2019) 3390–3400.
[20] Y. Sun, R. Fang, C. Li, L. Li, F. Li, X. Ye, et al., Hsa-mir-182 suppresses lung tumorigenesis through down regulation of RGS17 expression in vitro, Biochem. Biophys. Res. Commun. 396 (2) (2010) 501–507.
[21] Issue information-declaration of Helsinki, J. Bone Miner. Res. 34 (3) (2019) (BMi-BMii).
[22] M. El-Zein, L. Richardson, E.L. Franco, Cervical cancer screening of HPV vaccinated populations: cytology, molecular testing, both or none, J. Clin. Virol. 76 (Suppl. 1) (2016) S62–s8.
[23] M.J. Fan, Y.H. Zou, P.J. He, S. Zhang, X.M. Sun, C.Z. Li, Long non-coding RNA SPRY4-IT1 promotes epithelial-mesenchymal transition of cervical cancer by regulating the miR-101-3p/ZEB1 axis, Biosci. Rep. 39 (6) (2019).
[24] H. Zhao, G.H. Zheng, G.C. Li, L. Xin, Y.S. Wang, Y. Chen, et al., Long noncoding RNA LINC00958 regulates cell sensitivity to radiotherapy through RRM2 by binding to microRNA-5095 in cervical cancer, J. Cell. Physiol. 234 (12) (2019) 23349–23359.
[25] Q. Zhai, L. Zhou, C. Zhao, J. Wan, Z. Yu, X. Guo, et al., Identification of miR-508-3p and miR-509-3p that are associated with cell invasion and migration and involved in the apoptosis of renal cell carcinoma, Biochem. Biophys. Res. Commun. 419 (4) (2012) 621–626.
[26] W. Zhang, S. Qian, G. Yang, L. Zhu, B. Zhou, J. Wang, et al., MicroRNA-199 suppresses cell proliferation, migration and invasion by downregulating RGS17 in hepatocellular carcinoma, Gene 659 (2018) 22–28.
[27] Y. Chi, Q. Jin, X. Liu, L. Xu, X. He, Y. Shen, et al., miR-203 inhibits cell proliferation, invasion, and migration of non-small-cell lung cancer by downregulating RGS17, Cancer Sci. 108 (12) (2017) 2366–2372.